AGU PUBLICATIONS

Geophysical Research Letters

RESEARCH LETTER
10.1002/2015GL066903

Key Points:
- Tropical precipitation, monsoon jump, and hurricane frequency are all improved in HadGEM2-ES
- Equilibrating hemispheric albedos corrects the atmospheric cross-equatorial energy transport
- At a minimum, this suggests that models should tune against hemispheric albedo equivalence

Supporting Information:
- Figures S1–S9 and Table S1

Correspondence to:
J. M. Haywood,
jim.haywood@metoffice.gov.uk

Citation:
Haywood, J. M., et al. (2016), The impact of equilibrating hemispheric albedos on tropical performance in the HadGEM2-ES coupled climate model, *Geophys. Res. Lett., 43*, 395–403, doi:10.1002/2015GL066903.

Received 6 NOV 2015
Accepted 10 DEC 2015
Accepted article online 15 DEC 2015
Published online 14 JAN 2016

The impact of equilibrating hemispheric albedos on tropical performance in the HadGEM2-ES coupled climate model

Jim M. Haywood[1,2], Andy Jones[1], Nick Dunstone[1], Sean Milton[1], Michael Vellinga[1], Alejandro Bodas-Salcedo[1], Matt Hawcroft[2], Ben Kravitz[3], Jason Cole[4], Shingo Watanabe[5], and Graeme Stephens[6]

[1]Met Office Hadley Centre, Exeter, UK, [2]CEMPS, University of Exeter, Exeter, UK, [3]Atmospheric Sciences and Global Change Division, Pacific Northwest National Laboratory, Richland, Washington, USA, [4]Canadian Centre for Climate Modeling and Analysis, Environment Canada, Toronto, Ontario, Canada, [5]Japan Agency for Marine-Earth Science and Technology, Yokohama, Japan, [6]JPL, Pasadena, California, USA

Abstract The Earth's hemispheric reflectances are equivalent to within $\pm 0.2\,\mathrm{Wm}^{-2}$, even though the Northern Hemisphere contains a greater proportion of higher reflectance land areas, because of greater cloud cover in the Southern Hemisphere. This equivalence is unlikely to be by chance, but the reasons are open to debate. Here we show that equilibrating hemispheric albedos in the Hadley Centre Global Environment Model version 2-Earth System coupled climate model significantly improves what have been considered longstanding and apparently intractable model biases. Monsoon precipitation biases over all continental land areas, the penetration of monsoon rainfall across the Sahel, the West African monsoon "jump", and indicators of hurricane frequency are all significantly improved. Mechanistically, equilibrating hemispheric albedos improves the atmospheric cross-equatorial energy transport and increases the supply of tropical atmospheric moisture to the Hadley cell. We conclude that an accurate representation of the cross-equatorial energy transport appears to be critical if tropical performance is to be improved.

1. Introduction

The majority of global coupled atmosphere-ocean models do not replicate the observed hemispheric albedo equivalence [e.g., *Vonder Haar and Suomi*, 1971; *Ramanathan*, 1987; *Loeb et al.,* 2009; *Stevens and Schwartz*, 2012; *Voigt et al.,* 2013; *Stephens et al.,* 2015]; an analysis of models participating in the Coupled Model Intercomparison Project phase 3 (CMIP3) [*Taylor et al.,* 2012] suggests that 65% of the models exhibit a Northern Hemisphere albedo that is higher than the Southern Hemisphere [*Voigt et al.,* 2013]. When compared against measurements from the Clouds and the Earth's Radiant Energy System (CERES) sensor for the present day, Hadley Centre Global Environment Model version 2-Earth System (HadGEM2-ES), the coupled atmosphere-ocean Earth system model of the Met Office Hadley Centre [*Collins et al.,* 2011], reflects $3.8\,\mathrm{Wm}^{-2}$ more solar radiation from the Northern Hemisphere than the Southern Hemisphere mainly owing to biases in cloud representation at southern latitudes [*Bodas-Salcedo et al.,* 2014]. While the model is capable of accurately representing the observed historical evolution of global mean temperature under the influence of increasing concentrations of greenhouse gases and other climate forcing mechanisms [*Collins et al.,* 2011; *Jones et al.,* 2011], specific longstanding biases are evident in most tropical areas reflecting the model's inability to accurately represent processes that control tropical rainfall. The timing and magnitude of monsoons and tropical cyclone frequency are persistent model biases that require improvement and limit the robustness of model results in future climate impact scenarios [*Williams et al.,* 2012].

Here we focus on idealized simulations where we force symmetry in the hemispheric albedos in HadGEM2-ES by perturbing the Southern Hemisphere energy balance either by stratospheric aerosol loading (simulation *STRAT*), by increasing ocean albedo (simulation *OCEAN*), or by brightening cloud (simulation *CLOUD*). Such idealized studies obviously do not address the cause of the hemispheric biases within the model [*Bodas-Salcedo et al.,* 2014] but rather assess the potential improvement in model performance should these biases be reduced.

2. Methods

2.1. The HadGEM2-ES General Circulation Model

HadGEM2-ES is a fully coupled atmosphere-ocean climate model developed by the Met Office Hadley Centre. The atmospheric component has 38 levels extending to 40 km, with a horizontal resolution of 1.25° × 1.875° in latitude and longitude, respectively, equivalent to a surface resolution of about 208 km × 139 km at the equator, reducing to 120 km × 139 km at 55° latitude [*Collins et al*., 2011]. ES refers to the Earth System version, which includes coupling to a full tropospheric chemistry scheme, the terrestrial carbon cycle, and an ocean biogeochemistry scheme. Well-mixed greenhouse-gas concentrations are prescribed as are emissions of anthropogenic aerosols or their precursors, and aerosol direct and indirect effects are represented using the Coupled Large-scale Aerosol Simulator for Studies in Climate aerosol scheme [*Bellouin et al.,* 2011]. Tropospheric ozone is simulated by the model from surface and aircraft emissions of tropospheric ozone precursors and reactive gases. Stratospheric ozone is prescribed as monthly zonal/height fields. Land cover is simulated by the model's dynamic vegetation scheme. Natural climate forcings are represented by prescribing time-varying changes in total solar irradiance and monthly volcanic perturbations to stratospheric aerosol optical depth which are applied in four equal-area latitudinal bands [*Jones et al.,* 2011].

2.2. HadGEM2-ES Model Simulations and Analysis Periods

We perform four dedicated fully coupled simulations and analyze results over the 20 year period 1979–1998:

HIST. Historical simulation follows the CMIP5 [*Taylor et al.,* 2012] protocol using historical data from 1860 to 2005. The imbalance in the hemispheric energy budget is around 3.8 Wm^{-2} during this period, with the Northern Hemisphere being brighter than the Southern Hemisphere.

STRAT. We increase the Southern Hemisphere stratospheric aerosol optical depth by continually injecting 9.1 $TgSO_2$/yr across all latitudes of the Southern Hemisphere stratosphere, which increases the Southern Hemisphere aerosol optical depth at 550 nm by 0.18.

OCEAN. We increase Southern Hemisphere direct and diffuse ocean albedo by a factor of 1.875.

CLOUD. We increase the minimum cloud droplet number concentration over Southern Hemisphere ocean and land from 5 cm^{-3} and 35 cm^{-3}, respectively, to a value of 50 cm^{-3} for the whole Southern Hemisphere, which leads to a brightening of liquid-phase clouds. Ice clouds are not modified.

We emphasize that these three approaches are idealized and not intended to represent reality, but all balance the top of the atmosphere hemispheric reflectances over the period 1979–1998 to within the ±0.2 Wm^{-2} uncertainty evident in CERES observations [*Stephens et al.,* 2015].

In addition, we perform two simulations where the sea surface temperatures are fixed to their climatologically varying values (i.e., atmosphere-only simulations) and thus are not able to respond to the imposed external forcings:

HIST_FIXED_SST. As per *HIST*, but using climatologically varying sea surface temperatures (SSTs) used in Atmospheric Model Intercomparison Project studies [*Taylor et al.,* 2012]. The imbalance in the hemispheric energy budget in *HIST_FIXED_SST* is around 1.8 Wm^{-2}, with the Northern Hemisphere being brighter than the Southern Hemisphere, and thus, the imbalance is approximately half of *HIST*.

STRAT_FIXED_SST. As per *STRAT*, but again using climatological SSTs. As in *STRAT* the top of the atmosphere hemispheric reflectances over the period 1979–1998 is balanced to within ± 0.2 Wm^{-2}.

2.3. Data and Metrics for Assessing Model Performance

Our analysis of precipitation biases is based on Global Precipitation Climatology Project (GPCP) version 2 data [*Adler et al.,* 2003] over the period 1979–1998 for December–February, March–May, June–August (JJA), and September–November. Quantitative analysis focuses on land over specific regions (Figure S1 in the supporting information) [*Giorgi*, 2006]. Our analysis of the onset of the West African monsoon uses zonally averaged pentadal GPCP (1979–1998) precipitation data [*Adler et al.,* 2003; *Xie et al.,* 2003] and Tropical Rainfall Measuring Mission (TRMM) (1998–2010) daily accumulations of three hourly rainfall rates [*Simpson et al.,* 1988] averaged into 5 day means [*Xie et al.,* 2003; *Vellinga et al.,* 2013]. Although the TRMM data do not correspond to the exact time

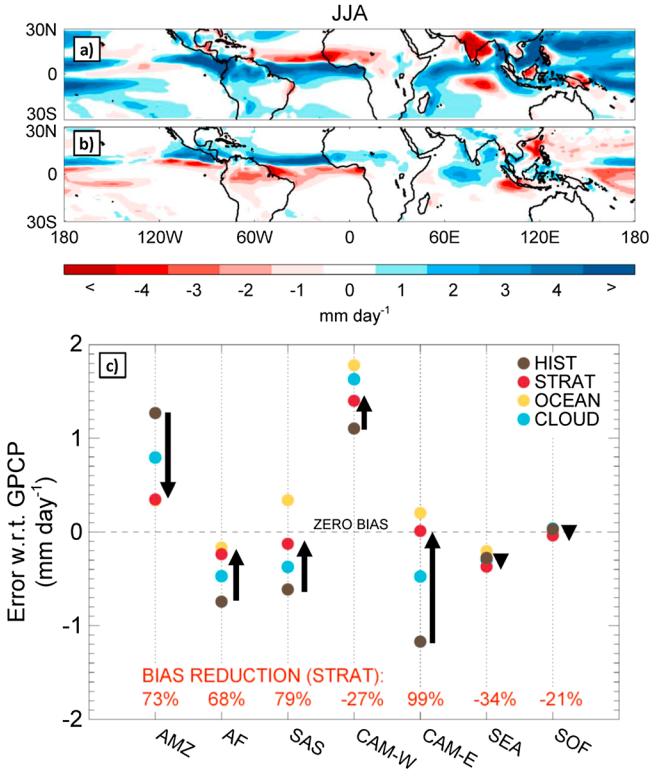

Figure 1. (a) The June–August (JJA) precipitation bias in HadGEM2-ES (mm day^{-1}) when compared against GPCP data (1979–1998). (b) The seasonal change in precipitation caused by equilibrating the hemispheric albedos in STRAT. (c) Quantitative assessment of the change in the bias with respect to GPCP for the JJA season over land in the following regions: AMZ: Amazonia, AF: Sahelian Africa, SAS: South Asia, CAM-W: Central America West, CAM-E: Central America East, SEA: South East Asia, SOF: Southern Africa (see supporting information in Figure S1 for these regions). The percentage change in the precipitation biases for *STRAT* compared to *HIST* are emphasized by black arrow and quantified for each region.

period of analysis, it is included because the use of radar measurements of precipitation makes it arguably the most accurate observational estimate.

The vertically integrated zonal-annual-mean northward moisture transport is calculated as [*Peixoto and Oort*, 1983] follows:

$$\mathrm{MTQ} = \frac{1}{p_*}\int_0^{p_*} \overline{vq}\,\mathrm{d}p \qquad (1)$$

where p_* is the surface pressure, v is the northward component of the wind speed, and q is the specific humidity and the units of MTQ are ms^{-1} g kg^{-1}.

Our analysis of hurricane frequency focuses on four metrics over the hurricane season (June–November) in the Maximum Development Region (MDR) defined by the area 10–20°N in the tropical Atlantic Ocean: MDR wind shear (vertical wind-shear between 250 hPa and 850 hPa), MDR precipitation, and the Tropical Storm Index [*Knutson et al.*, 2010]. Model performance is assessed using different sources of data: MDR wind shear is compared against European Centre Re-Analyses Interim (ERA-Interim) data [*Dee et al.*, 2011], MDR rainfall is compared against GPCP data [*Tebaldi and Knutti*, 2007], and the Tropical Storm Index is derived as the difference between the MDR sea surface temperature and tropical-averaged sea surface temperature.

3. Results

One major impact should be a northward shift in the Intertropical Convergence Zone (ITCZ), as previously noted in HadGEM2-ES [*Haywood et al.*, 2013], idealized aqua-planet simulations [*Kang et al.*, 2009; *Voigt et al.*, 2013, 2014], and multimodel analysis of CMIP5 models [*Hwang and Frierson*, 2013]. Therefore, we initially focus on tropical precipitation during the June–August (JJA) season when the Northern Hemisphere monsoon is most active.

Figure 1a shows the precipitation biases over many areas of the tropics in the historical simulation (*HIST*) when compared against GPCP observations [*Adler et al.*, 2003]. The long-standing dry bias in Sahelian Africa and the Indian subcontinent are evident, while a wet bias exists over the Amazonian region. Figure 1b shows that equilibrating hemispheric albedos in *STRAT* almost universally reduces precipitation biases for JJA, while Figure 1c shows a quantitative reduction in dry bias by 79% for South Asia (SAS) and 68% for the Sahel (AF), while the wet bias over Amazonia (AMZ) is reduced by 73%.

For HadGEM2-ES biases exist across all seasons in *HIST*, but equilibrating the hemispheric albedos leads to a significant compensation (supporting information Figure S2). Supporting information Table S1 shows quantitative analysis of the change in the precipitation bias over climatological hot spot areas [*Giorgi*, 2006] for

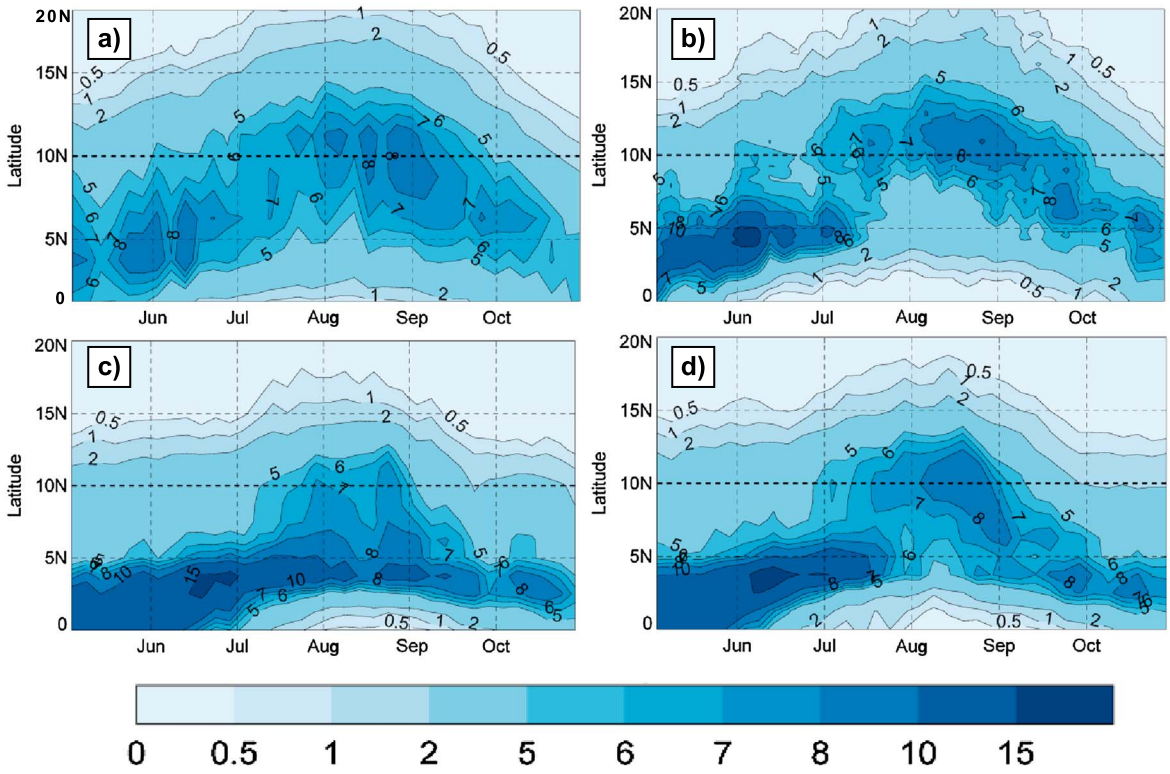

Figure 2. The temporal and latitudinal evolution of zonally averaged (10°E–10°W) west African precipitation (mm day^{-1}) from (a) GPCP, (b) TRMM, (c) *HIST*, and (d) *STRAT* simulations. The analysis is performed for the 1979–1998 period. The 10°N latitude is frequently used as an indicator for the monsoon jump and is highlighted by the bold dashed horizontal line.

STRAT, *OCEAN*, and *CLOUD* simulations. All three simulations produce broadly similar spatial patterns in precipitation change, although *OCEAN* has the strongest impacts, *CLOUD* the weakest, and *STRAT* an intermediate impact (supporting information Table S1). Henceforth, we focus on *STRAT* (i.e., intermediate impacts). In all three simulations, the impact on precipitation in the extratropics is minor and is not shown here.

We also compare the hemispherically equilibrated coupled climate simulations against simulations from a similarly equilibrated atmosphere-only version of the model with prescribed sea surface temperatures (SSTs). We find that equilibrating hemispheric albedos has little impact on the simulations that use fixed SSTs but also that the coupled model performs significantly better in terms of precipitation performance (section 2 and supporting information Figure S3). This suggests that inhibiting the interaction between atmosphere and ocean prevents the improvement in precipitation evident in the fully coupled model. Additionally, equilibrating the hemispheric albedos in the coupled model leads to a model that performs better in terms of tropical precipitation over land than the atmosphere-only model with ostensibly perfect SSTs. By construction, fixed SST simulations cannot adjust the sensible and latent heat components from the ocean to the atmosphere when exposed to an external forcing and cannot adequately represent changes in the atmospheric energy flows that are observed in *STRAT*.

Equilibrating the hemispheric albedos also impacts the timing of the West African monsoon. Following previous studies [*Vellinga et al.,* 2013], Figure 2 shows the temporal evolution of zonally averaged precipitation data from GPCP [*Xie et al.,* 2003] and TRMM [*Simpson et al.,* 1988] along with results from *HIST* and *STRAT* simulations.

Monsoon onset is characterized by a rapid northward shift in rainfall maxima in early July from the Gulf of Guinea coast to the Sahel/Sudan (Figures 2a and 2b) [*Vellinga et al.,* 2013; *Sultan and Janicot*, 2003]. This monsoon "jump" of precipitation from latitudes south of 5°N to north of 10°N is not evident in the *HIST* simulation (Figure 2c) but is relatively well represented in STRAT (Figure 2d). Thus, equilibrating the hemispheric albedo significantly improves model performance in this key area [*Williams et al.,* 2012] and appears to be linked to an increased supply of atmospheric moisture that penetrates into the interior of the African continent. In *STRAT*, over ocean the increase/decrease in precipitation is strongly correlated

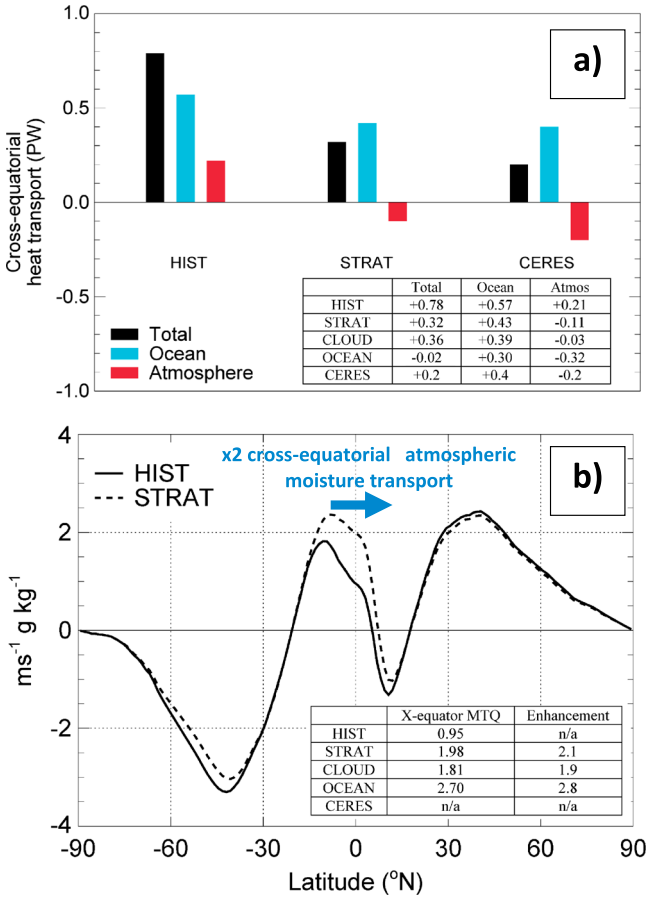

	Total	Ocean	Atmos
HIST	+0.78	+0.57	+0.21
STRAT	+0.32	+0.43	-0.11
CLOUD	+0.36	+0.39	-0.03
OCEAN	-0.02	+0.30	-0.32
CERES	+0.2	+0.4	-0.2

	X-equator MTQ	Enhancement
HIST	0.95	n/a
STRAT	1.98	2.1
CLOUD	1.81	1.9
OCEAN	2.70	2.8
CERES	n/a	n/a

Figure 3. (a) A summary of the northwards cross-equatorial energy transport (PW) from the *HIST* and *STRAT* simulations over the 1979–1998 period. The observed energy transport derived from CERES is also shown. Tabulated values also give the cross-equatorial energy transport (PW) from the *OCEAN* and *CLOUD* simulations. (b) The annual-mean meridional transport of moisture (MTQ, ms^{-1} g kg^{-1}, from equation (1)). Positive values represent northward transport, while negative values represent southward transport. Tabulated values give the cross-equatorial meridional transport of moisture (MTQ, ms^{-1} g kg^{-1}) and enhancement from the *HIST*, *STRAT*, *OCEAN*, and *CLOUD* simulations.

withthe increase/decrease in moisture convergence (supporting information Figure S4a), a correlation which is also apparent over South America. Over the Sahel, the situation is more complex; the anticyclonic wind field perturbation centered over southern Mali leads to a decrease in moisture convergence although the precipitation increases. Similar responses have been noted in simulations using the Met Office Unified model at higher resolutions [*Birch et al.,* 2014]. The change in the moisture convergence in *OCEAN* and *CLOUD* exhibits very similar spatial patterns to *STRAT*, but the cross-equatorial atmospheric moisture supply is larger under *OCEAN* and smaller under *CLOUD* than in the *STRAT* simulations (supporting information Figures S4b and S4c).

We examine the atmospheric and oceanic energy terms which are diagnosed explicitly in the ocean model and derived as the difference between the top of atmosphere net radiation and the surface energy budget for the atmosphere [*Trenberth and Caron*, 2001; *Vellinga and Wu*, 2008] (supporting information Figure S5). While changes in the total transport of energy appear relatively subtle, the change in the cross-equatorial energy transport is significant (Figure 3a).

In *HIST* there is a significant net northward cross-equatorial energy transport of approximately +0.78 Peta Watts (PW, 10^{15} w) (+0.57 PW from ocean and +0.21 PW from the atmosphere). This is contrary to observational estimates from CERES which suggest +0.2 PW in total (+0.4 PW from the ocean and −0.2 PW from the atmosphere) [*Voigt et al.,* 2013; *Stephens et al.,* 2015]. Thus, in *HIST* the atmosphere is transporting energy from the Southern Hemisphere to the Northern Hemisphere (i.e., in the wrong direction). In *STRAT* the total is +0.32 PW (+0.43 PW from ocean, and −0.11 PW from the atmosphere) with both the model atmosphere and ocean transporting energy in the correct directions. The results from *OCEAN* and *CLOUD* also correct the sign of the atmospheric cross-equatorial atmospheric energy transport as shown in Figure 3a.

Idealized aqua-planet simulations clearly demonstrate that low-level moisture transport in the atmospheric Hadley cell opposes the atmospheric energy transport [*Voigt et al.,* 2013, 2014; *Frierson et al.,* 2013]. Obviously, aqua-planet configurations cannot be used to quantify the impact of equilibrating hemispheric albedos on model performance (e.g., in continental precipitation and the African monsoon jump), as they do not include continents of any kind. However, in our fully coupled model simulations, the increased northward supply of atmospheric tropical moisture seen in aqua-planet simulations is clearly evident in the vertically integrated zonal-annual-mean moisture transport (MTQ) [*Peixoto and Oort*, 1983] (Figure 3b). The cross-equatorial MTQ is enhanced by a factor of 2.1 in the *STRAT* simulations, increasing the moisture supply to the Northern Hemisphere. The *OCEAN* and *CLOUD* simulations lead to a

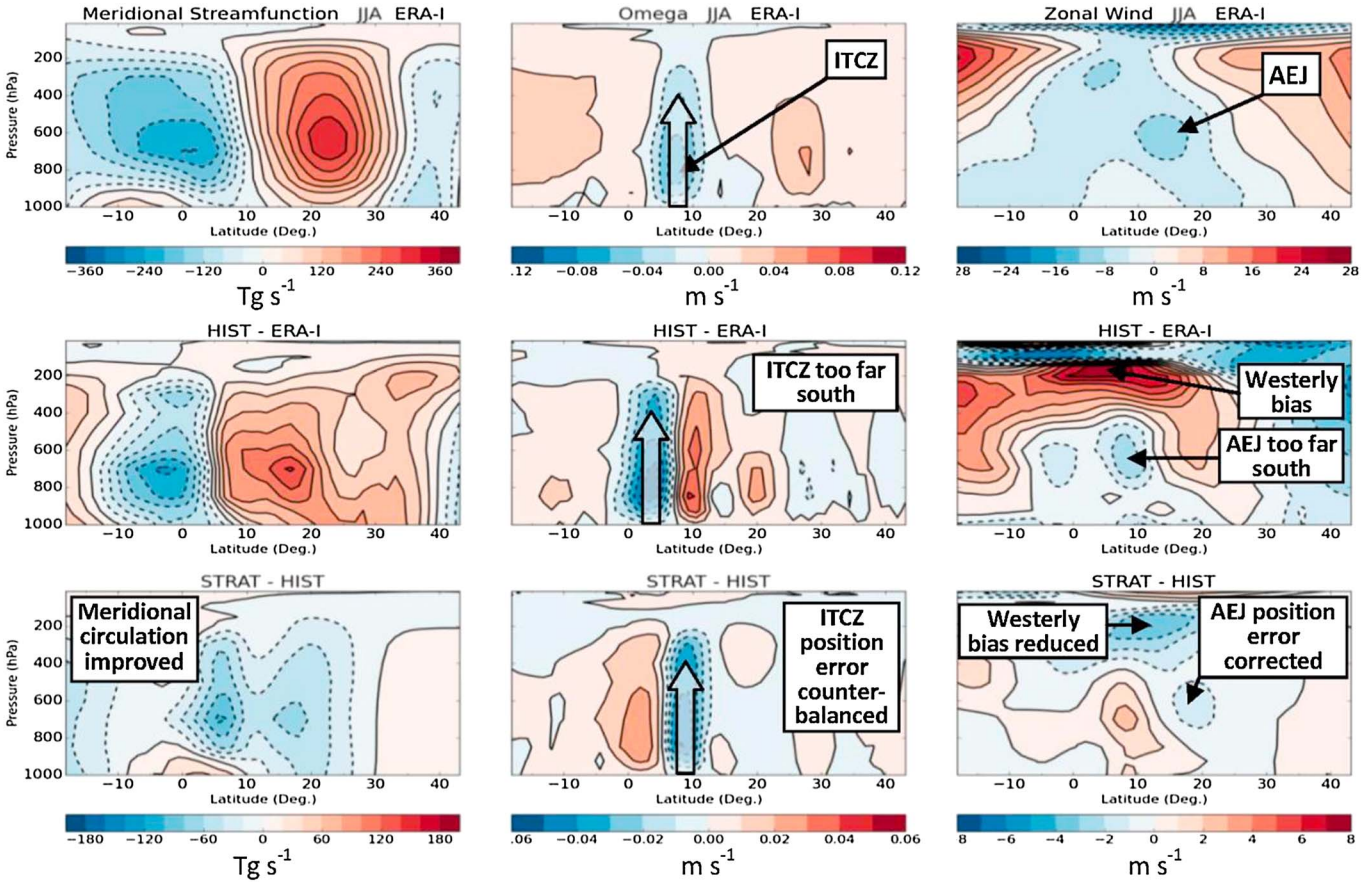

Figure 4. The impacts on Tropical Atlantic and West Africa monsoon circulations for JJA 1979–1998 using data averaged from 60°W to 0°E. Column 1: latitude-pressure sections of mass meridional stream function (10^{12} g s^{-1}), column 2: vertical velocity (m s^{-1}), and column 3: zonal wind (m s^{-1}) for (first row) ERA-Interim reanalysis, (second row) error in *HIST* (*HIST-ERA*), and (third row) differences between the two experiments (*STRAT-HIST*). The opaque arrows in the second column represent the approximate position of the ITCZ.

somewhat larger (a factor of 2.9) and somewhat smaller response (a factor of 1.9) respectively consistent with the magnitude of the tropical precipitation response in each simulation (Figure 1c).

To further investigate the mechanism of these improvements we focus on changes in the dominant dynamical features: the zonal tropical overturning circulation and the African easterly jet (AEJ), which are maintained by two diabatically forced meridional circulations, one associated with deep moist convection in the ITCZ and a second from dry convection to the north over the Sahara [*Thorncroft and Blackburn*, 1999].

Figure 4 examines the June–August 1979–1998 mean tropical circulation in the Atlantic and West African region (60°W–0°E), where large reductions in precipitation bias are evident when hemispheric albedos are equilibrated. Comparing *HIST* with ERA-Interim reanalyses (second row, first and second column) shows a systematic southward bias (up to 5°) of the ITCZ and region of maximum vertical ascent, consistent with the pattern of precipitation biases in *HIST*. This is accompanied by a southward bias in the AEJ at 700 hPa and a large westerly bias in the tropical upper troposphere at 200 hPa (second row, third column). The *STRAT* simulation counterbalances errors in the meridional circulation at 0–20°N (third row, first column) and the position of the ITCZ and maximum vertical ascent (third row, second column). The representation of the AEJ is improved (third row, third column), and the excessive westerly winds in the upper troposphere in *HIST* are also reduced in *STRAT* due to reduction of the erroneous poleward transport in upper levels of the mean meridional circulation (5–20°N).

Another key bias in HadGEM2-ES is low hurricane frequency and intensity [*Williams et al.*, 2012]. HadGEM2-ES (~200 km equatorial resolution) cannot adequately represent the central pressure of hurricanes, but metrics for coarse resolution models as indicators of hurricane frequency have been developed that may be compared against suitably averaged observations focused on the Maximum Development Region

(MDR; 10°N–20°N in the tropical Atlantic) for tropical hurricanes [e.g., *Smith et al.,* 2010; *Knutson et al.,* 2010; *Dunstone et al.,* 2013]. Equilibrating the hemispheric albedos in *STRAT* reduces biases in MDR wind shear (owing to the reduction in the westerly bias in the tropical upper troposphere shown in Figure 4), precipitation (owing to the increase in the precipitation shown in Figure 1b), and the tropical storm index (see supporting information Figure S6), by 58%, 82%, and 52%, respectively, when compared to the observational/reanalysis products, indicating a significant improvement in model performance. While there have been idealized aqua-planet simulations that perturb oceanic cross equatorial energy transport and assess the impacts on hurricane frequency [*Merlis et al.,* 2013], our fully coupled simulations indicate that representing the atmospheric cross equatorial energy transport is also important if hurricane frequency is to be accurately modeled in future climate simulations [*Knutson et al.,* 2010].

4. Discussion and Conclusions

Our results suggest that, in HadGEM2-ES, equilibrating hemispheric albedos by various idealized methods corrects the direction of atmospheric cross-equatorial energy transport, which increases the northward cross-equatorial atmospheric moisture supply to the ITCZ leading to significant improvements in the representation of tropical precipitation. This mechanistic link has been demonstrated in aqua-planet simulations [*Kang et al.,* 2009; *Frierson et al.,* 2013; *Voigt et al.,* 2014] and in models with realistic geography [*Frierson et al.,* 2013], but these studies did not make comparisons against synergistic observations to assess model performance. Our simulations show that the model response in each of the three idealized methods (*STRAT*, *CLOUD*, and *OCEAN*) are broadly similar indicating that the results are unlikely to be a side effect of our methodology. As the *STRAT*/*CLOUD*/*OCEAN* simulations initiate additional reflection of solar radiation in the stratospheric/boundary layer/surface, the results appear relatively insensitive to the vertical location of the energy perturbation.

We note that multimodel assessments of the impact of meridional gradients in planetary albedo have focused on the impacts on zonal SST gradients [e.g., *Burls and Fedorov*, 2014]. A particularly relevant study is that of *Hwang and Frierson* [2013] (HF13), who showed a striking relationship between the "precipitation asymmetry index" (defined as model precipitation over the latitudinal range 0–20°N minus that for 0–20°S normalized by the mean tropical precipitation over 20°N–20°S) and cross-equatorial energy transport in CMIP5 models. An analysis of *HIST*, *STRAT*, *CLOUD*, and *OCEAN* (supporting information, Figure S9) indicates that the striking linear relationship shown in the multimodel ensemble of HF13 is also evident in our simulations with a gradient of −1.5 PW per unit HF13 precipitation asymmetry index which is very similar to that found in HF13. There is also a similar relationship between the cross-equatorial energy transport and the H15 asymmetry index (see supporting information, Figure S9) which is more relevant for the analyses we present in this study. As in HF13, in HadGEM2-ES the precipitation asymmetry index is close to zero when the interhemispheric temperature asymmetry is close to zero although the interhemispheric temperature asymmetry per unit HF13 precipitation asymmetry index is less in HadGEM2-ES. This analysis suggests the HadGEM2-ES simulations appear representative of the multimodel ensemble suggesting that other models may well respond in a similar way to HadGEM2-ES. Future work should therefore focus on the results from multiple models, but we note that use of CMIP5 data from standard scenarios will not capture the change in the performance of an individual model under hemispheric albedo equalization. Multiple model simulations equilibrating the hemispheric albedos are suggested to investigate the robustness of these findings.

While equilibrating hemispheric albedos in HadGEM2-ES improves the tropical performance of the model when assessed against observations, there are important caveats that need to be considered. First, *STRAT* leads to deterioration in the representation of tropical SSTs which are too cold even in *HIST* (supporting information Figure S7). Forcing the Southern Hemisphere to cool in *STRAT* increases the bias further. Thus, while we are able to reduce the monsoon precipitation biases in *STRAT*, we replace a systematic bias in precipitation with a systematic bias in SSTs. However, we can identify a reason for the improvement in African and South American monsoon precipitation by analyzing the gradient of tropical SSTs in *HIST* and *STRAT* with respect to observations. Across the latitude range 20°N–20°S the gradient in the Atlantic SSTs from *STRAT* are in better agreement with the observations than those from *HIST* (supporting information Figure S8). The observations suggest a relatively weak/strong gradient northward/southward of the peak in normalized SSTs compared to the *HIST* simulation. This error is corrected in *STRAT*. Gradients of SST have been implicated as strong drivers

of Sahelian precipitation for some time [*Zeng*, 2003; *Folland et al.,* 1986] but, with the exception of HF13, the link to the hemispheric energy balance has not previously been established. Indeed, accurate representation of SSTs and SST gradients does not necessarily lead to accurate representation of tropical precipitation as emphasized by the *HIST_FIXED_SST* and *STRAT_FIXED_SST* atmosphere-only simulations performed here. The fully coupled *STRAT* simulation where the SST gradients and the atmospheric cross-equatorial transport are in approximate agreement with observations provides a better representation of tropical precipitation. This suggests limitations to the approach of driving models using fixed SSTs; in HadGEM2-ES, fully coupled model simulations are required if the atmospheric energy transport is to be accurately represented with implications for accurate representation of tropical precipitation.

A further caveat is that our idealized study does not tackle the issue of how to realistically achieve an accurate representation of hemispheric albedo balance, which should be a topic of further research, but it shows the considerable potential improvement in representation of tropical precipitation and hurricane frequency if that is achieved. Future work should include assessment of the impacts of equilibrating not just the gross hemispheric albedo but evaluating the impacts of reducing the zonal mean and spatial distribution of albedo biases and, of course, trying to tackle the root cause of these biases [*Bodas-Salcedo et al.,* 2014].

Acknowledgments

J.M.H., M.H., S.M., and M.V. were part funded by the IMPALA grant (NE/M017214/1) via Future Climates for Africa (FCFA) funding provided by NERC and DFID. J.M.H., A.J., N.D., S.M., and M.V. were supported by the Joint UK DECC/Defra Met Office Hadley Centre Climate Programme (GA01101). B.K. is supported by the Fund for Innovative Climate and Energy Research (FICER). PNNL is operated for the U.S. Department of Energy by Battelle Memorial Institute under contract DE-AC05-76RL01830. Data availability: HadGEM2-ES is a fully coupled GCM with a heritage that is well documented. Owing to the complexities of running simulations on high-performance computing equipment, the code is not generally available. Data from the model are freely available by contacting J.M.H. directly (j.m.haywood@exeter.ac.uk).

References

Adler, R. F., et al. (2003), The version-2 global precipitation climatology project (GPCP) monthly precipitation analysis (1979-present), *J. Hydrometeorol.*, *4*(6), 1147–1167.

Bellouin, N., J. Rae, A. Jones, C. Johnson, J. M. Haywood, and O. Boucher (2011), Aerosol forcing in the CMIP5 simulations by HadGEM2-ES and the role of ammonium nitrate, *J. Geophys. Res.*, *116*, D20206, doi:10.1029/2011JD016074.

Birch, C. E., D. J. Parker, J. H. Marsham, D. Copsey, and L. Garcia-Carreras (2014), A seamless assessment of the role of convection in the water cycle of the West African monsoon, *J. Geophys. Res. Atmos.*, *119*, 2890–2912, doi:10.1002/2013JD020887.

Bodas-Salcedo, A., K. D. Williams, M. A. Ringer, I. Beau, J. N. S. Cole, J.-L. Dufresne, T. Koshiro, B. Stevens, Z. Wang, and T. Yokohata (2014), Origins of the solar radiation biases over the Southern Ocean in CFMIP2 Models, *J. Clim.*, *27*(1), 41–56.

Burls, N. J., and A. V. Fedorov (2014), What controls the mean east–west sea surface temperature gradient in the equatorial Pacific: The role of cloud albedo, *J. Clim.*, *27*, 2757–2778, doi:10.1175/JCLI-D-13-00255.1.

Collins, W. J., et al. (2011), Development and evaluation of an Earth-system model—HadGEM2, *Geosci. Model Dev.*, *4*, 1051–1075, doi:10.5194/gmd-4-1051-2011.

Dee, D. P., et al. (2011), The ERA-Interim reanalysis: Configuration and performance of the data assimilation system, *Q. J. R. Meteorol. Soc.*, *137*(656), 553–597.

Dunstone, N. J., D. M. Smith, B. B. B. Booth, L. Hermanson, and R. Eade (2013), Anthropogenic aerosol forcing of Atlantic tropical storms, *Nat. Geosci.*, *6*(7), 534–539.

Folland, C. K., T. N. Palmer, and D. E. Parker (1986), Sahel rainfall and worldwide sea temperatures, 1901_85, *Nature*, *320*, 602–607.

Frierson, D. M., Y.-T. Hwang, N. S. Fučkar, R. Seager, S. M. Kang, A. Donohoe, E. A. Maroon, X. Liu, and D. S. Battisti (2013), Contribution of ocean overturning circulation to tropical rainfall peak in the Northern Hemisphere, *Nat. Geosci.*, *6*(11), 940–944.

Giorgi, F. (2006), Climate change hot-spots, *Geophys. Res. Lett.*, *33*, L08707, doi:10.1029/2006GL02573.

Haywood, J. M., A. Jones, N. Bellouin, and D. B. Stephenson (2013), Asymmetric forcing from stratospheric aerosols impacts Sahelian drought, *Nat. Clim. Change*, *3*(7), 660–665, doi:10.1038/NCLIMATE1857.

Hwang, Y. T., and D. M. Frierson (2013), Link between the double-intertropical convergence zone problem and cloud biases over the Southern Ocean, *Proc. Natl. Acad. Sci. U.S.A.*, *110*(13), 4935–4940.

Jones, C. D., et al. (2011), The HadGEM2-ES implementation of CMIP5 centennial simulations, *Geosci. Model Dev.*, *4*, 543–570, doi:10.5194/gmd-4-543-2011.

Kang, S. M., D. M. Frierson, and I. M. Held (2009), The tropical response to extratropical thermal forcing in an idealized GCM: The importance of radiative feedbacks and convective parameterization, *J. Atmos. Sci.*, *66*(9), 2812–2827.

Knutson, T. R., J. L. McBride, J. Chan, K. Emanuel, G. Holland, C. Landsea, I. Held, J. P. Kossin, A. K. Srivastava, and M. Sugi (2010), Tropical cyclones and climate change, *Nat. Geosci.*, *3*, 157–163.

Loeb, N. G., B. A. Wielicki, D. R. Doelling, G. L. Smith, D. F. Keyes, S. Kato, N. Manalo-Smith, and T. Wong (2009), Toward optimal closure of the Earth's top-of-atmosphere radiation budget, *J. Clim.*, *22*, 748–766.

Merlis, T. M., M. Zhao, and I. M. Held (2013), The sensitivity of hurricane frequency to ITCZ changes and radiatively forced warming in aquaplanet simulations, *Geophys. Res. Lett.*, *40*, 4109–4114, doi:10.1002/grl.50680.

Peixoto, J. P., and A. H. Oort (1983), The atmospheric branch of the hydrological cycle and climate, in *Variations in the Global Water Budget*, pp. 5–65, Springer, Netherlands.

Ramanathan, V. (1987), The role of Earth radiation budget studies in climate and general circulation research, *J. Geophys. Res.*, *92*(D4), 4075–4095, doi:10.1029/JD092iD04p04075.

Simpson, J., R. Adler, and G. North (1988), A proposed tropical rainfall measuring mission (TRMM) satellite, *Bull. Am. Meteorol. Soc.*, *69*(3), 278–295.

Smith, D. M., R. Eade, N. J. Dunstone, D. Fereday, J. M. Murphy, H. Pohlmann, and A. A. Scaife (2010), Skilful multi-year predictions of Atlantic hurricane frequency, *Nat. Geosci.*, *3*(12), 846–849.

Stephens, G. L., D. O'Brien, P. J. Webster, P. Pilewski, S. Kato, and J.-l. Li (2015), The Albedo of Earth, *Rev. Geophys.*, *53*, 141–163, doi:10.1002/2014RG000449.

Stevens, B., and S. E. Schwartz (2012), Observing and modeling Earth's energy flows, *Surv. Geophys.*, *33*(3–4), 779–816.

Sultan, B., and S. Janicot (2003), The West African monsoon dynamics. Part II: The "preonset" and "onset" of the summer monsoon, *J. Clim.*, *16*, 3407–3427.

Taylor, K. E., R. J. Stouffer, and G. A. Meehl (2012), An overview of CMIP5 and the experiment design, *Bull. Am. Meteorol. Soc.*, *93*, 485–498.

Tebaldi, C., and R. Knutti (2007), The use of the multi-model ensemble in probabilistic climate projections, *Philos. Trans. R. Soc. A*, *365*(1857), 2053–2075.
Thorncroft, C. D., and M. Blackburn (1999), Maintenance of the African easterly jet, *Q. J. R. Meteorol. Soc.*, *125*(555), 763–786.
Trenberth, K. E., and J. M. Caron (2001), Estimates of meridional atmosphere and ocean heat transports, *J. Clim.*, *14*(16), 3433–3443.
Vellinga, M., and P. Wu (2008), Relations between northward ocean and atmosphere energy transports in a coupled climate model, *J. Clim.*, *21*, 561–575.
Vellinga, M., A. Arribas, and R. Graham (2013), Seasonal forecasts for regional onset of the West African monsoon, *Clim. Dyn.*, *40*, 3047–3070, doi:10.1007/s00382-012-1520-z.
Voigt, A., B. Stevens, J. Bader, and T. Mauritsen (2013), The observed hemispheric symmetry in reflected shortwave irradiance, *J. Clim.*, *26*(2), 468–477.
Voigt, A., B. Stevens, J. Bader, and T. Mauritsen (2014), Compensation of hemispheric albedo asymmetries by shifts of the ITCZ and tropical clouds, *J. Clim.*, *27*(3), 1029–1045.
Vonder Haar, T. H., and V. E. Suomi (1971), Measurements of the Earth's radiation budget from satellites during a five-year period. Part I: Extended time and space means, *J. Atmos. Sci.*, *28*, 305–314.
Williams, K., et al. (2012), Assessment of GA4/GL4/GO4/GSI4 and progress in addressing key model biases, Hadley Centre Technical Note, Sept. [Available at http://www.metoffice.gov.uk/media/pdf/c/l/AdditionalPaper_GA4_assessment.pdf.]
Xie, P. P., J. E. Janowiak, P. A. Arkin, R. Adler, A. Gruber, R. Ferraro, G. J. Huffman, and S. Curtis (2003), GPCP pentad precipitation analyses: An experimental dataset based on gauge observations and satellite estimates, *J. Clim.*, *16*(13), 2197–2214.
Zeng, N. (2003), Drought in the Sahel, *Science*, *302*, 999–1000.